

Bond performance of a lapping joint developed for precast concrete columns

R. Yanez & H. Imai

University of Tsukuba, Ibaraki, Japan

T. Yamaguchi

Kabuki Construction Co., Ltd, Tokyo, Japan

ABSTRACT: An experimental investigation was carried out in order to predict the bond behavior of a newly developed lapping joint for Precast Concrete (PCa) Columns. Pull out test on 27 specimens was carried out. Each one of the specimens represented the confined section of PCa columns, where steel sheaths were placed at the main bar positions and lapped with two bars each, and then, the main bars were inserted from the both sides of the sheath, so each main bar abutted at the middle height of the column specimens and high strength mortar was grouted inside. In this paper, the influences of the height of sheath lug, thickness of cover concrete, lateral reinforcement ratio, lapping length, and loading history on the bond performance of the lapping joints are investigated.

1. INTRODUCTION

One of the most important part in the design of Precast Concrete (PCa) structures is the connection details. Connections between precast members must effectively integrate the individual structural members in full continuity with each other so that the overall building structure behaves monolithically. Hitherto, in the conventional PCa methods, the main bars are placed inside of the PCa members and jointed at the same place where the PCa members are jointed too. This method generated a problem between the construction of precast members and the seismic performance because the main bars

are jointed where the stresses due to seismic forces are large.

A new concept was proposed by Imai (Imai 1991), based on that the main bars are not placed when the precast members are prefabricated and also that the bar joints are located at the middle part of each member, where the stresses due to the seismic forces are small.

A cheaper and simple joint method for PCa columns has been developed, which is used at the middle part of the members where the stresses are small, as Figure 1 shows. At the position of main bars, a sheath is placed and lapped with two bars each, then at the construction site the main bars are inserted into the sheaths, so the end of each bar abuts at the center of columns, and high strength mortar is grouted inside of the sheaths. The stress transfer mechanism of the lapping joint method is that the stress of main bar is transferred progressively to the mortar and then to the half part of the lapping bars through the sheath by bond stresses, and from the other half part of lapping bars to the other main bar, reversely.

The behavior of the main bar-mortar-sheath-lapping bars system to realize the above mentioned idea, is primarily governed by the interfacial bond characteristics between them. So, the bond strength of this lapping joint was studied in the pullout tests.

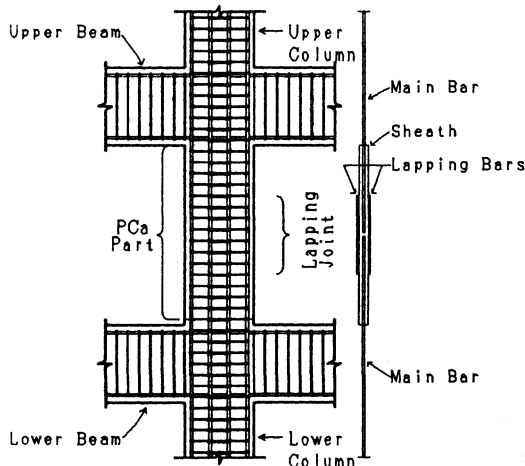


Figure 1. Proposed joint method

2. SPECIMEN

The test specimens were designed to

Table 1. Differences among specimens

| Parameter | Specimen | Height of Lug (mm) | Lateral Reinf. | Cover of Concrete (mm) | Specified Fc (kgf/cm ²) | Lapping Length |
|----------------------|----------------------------------|--------------------|----------------------------------|------------------------|-------------------------------------|----------------|
| Height of Sheath Lug | PS15 PS20 PS30 | 1.5 2.0 3.0 | 4-D10 | 40 | 300 | 20 d |
| Lateral Reinf. | PH210 PH410 PH413 PH416 | | 2-D10 4-D10 4-D13 4-D16 | | | |
| Cover of Concrete | PL20 PL30 PL40 | 2.0 | 4-D10 | 20 30 40 | | |
| Loading History | PR11 PR13 PR15 | | | 40 | | |

Sheath Diameter: 44 mm
 Main Bars: D25 (SD390)
 Lapped Bars: 2-D19 (SD390)
 Hoop: welded close type at every 100 mm
 d: lapping bar diameter

Table 2. Properties of steel

| Size | Grade | σ_y (tf/cm ²) | σ_u (tf/cm ²) | E (tf/cm ²) |
|------|--------|----------------------------------|----------------------------------|-------------------------|
| D10 | SD295A | 3.80 | 5.13 | 1914 |
| D13 | | 3.68 | 5.11 | 1835 |
| D16 | | 3.66 | 5.23 | 1919 |
| D19 | | 4.25 | 5.97 | 1890 |
| D25 | SD390 | 4.30 | 6.09 | 1972 |

Table 4. Properties of concrete

| Specimen | Specified Strength (kgf/cm ²) | Specimen Strength | |
|--|---|--------------------------------|---------------------------------|
| | | 4 Weeks (kgf/cm ²) | Exp. day (kgf/cm ²) |
| PS15 PS20 PS30 PH413 PH416 | 300 | 311 | 317 |
| PH210 PC20 PC30 | | | 326 |
| PR11 PR13 PR15 | | | |

represent a confined section of PCA columns. Figure 2 shows the detailed section of precast specimens and Table 1 shows the differences among the test specimens. The specified concrete strength for the PCA specimens was $F_c = 300 \text{ kgf/cm}^2$. Also the specified compressive strength of the grout mortar was 600 kgf/cm^2 . For main bars D25 with specified yield strength of 4000 kgf/cm^2 (SD390), and as lapped bars two

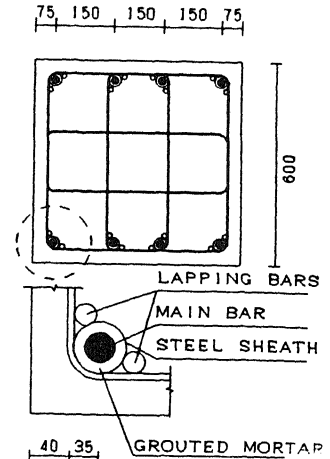


Figure 2. Section of specimen

Table 3. Properties of mortar

| Specified Strength (kgf/cm ²) | Grouting Day | Specimen Strength | | |
|---|--------------|-------------------------------|--------------------------------|---------------------------------|
| | | 7 Days (kgf/cm ²) | 4 Weeks (kgf/cm ²) | 13 Weeks (kgf/cm ²) |
| 600 | 11/3/91 | 548 | 668 | 748 |
| | 18/3/91 | 517 | 638 | 715 |

bars of D19 (SD390) were chosen for this investigation. Tables 2, 3 and 4 show the properties of the materials. The specimens were cast horizontally.

Depending on the parameter the specimens were divided into four cases: lug height of sheath, thickness of cover concrete, amount of lateral reinforcement, and loading history.

A steel spiral sheath of 44 mm diameter with lug height of 2 mm were used for all specimens except when the lug height was the parameter. Also, a cover concrete of 40 mm from the surface to the lateral reinforcement was considered for all specimens, except when the influence of the cover concrete was investigated. Each specimen had 4-D10 (SD295A) as lateral reinforcement, except when its influence on the joint was tested. As lapping length, 20 times the diameter of the lapping bar, 20d, was considered for all the PCA specimens.

3. TEST APPARATUS AND LOADING HISTORY

The loading arrangement is shown in Figure 3. Tension P was applied horizontally to both ends of the main bars by oil jacks controlled by a load cell. Displacements between both ends of the main bars were also measured.

In order to obtain the maximum load, monotonic load was applied to 22 specimens

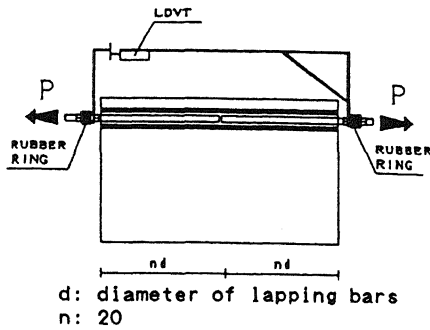


Figure 3. Loading system

with incremental of 1 tonf until failure. In case of the bottom bars, the maximum load was obtained after the bars yielded. The top bars did not yield before bond failure.

Table 5. Summary of test results

| Specimen | τ_{uexp} (kg/cm ²) | | τ_{ucm} (kg/cm ²) (Fujii et al) | τ_{ucoj} (kg/cm ²) (Orangun et al) |
|----------|--|-------|---|--|
| | 1 | 2 | | |
| PS15T | 35.90 | 37.27 | 29.14 | 33.97 |
| PS15B | 47.37 | 44.08 | 35.55 | 44.16 |
| PS20T | 34.00 | 35.87 | 29.14 | 33.97 |
| PS20B | 49.19 | 48.39 | 35.55 | 44.16 |
| PS30T | 34.03 | 37.67 | 29.14 | 33.97 |
| PS30B | 53.28 | 52.73 | 35.55 | 44.16 |
| PC20T | 29.99 | 33.93 | 29.56 | 29.19 |
| PC20B | 45.30 | 50.38 | 36.06 | 37.94 |
| PC30T | 37.35 | 35.87 | 29.56 | 31.82 |
| PC30B | 51.31 | 51.93 | 36.06 | 41.36 |
| PC40T | 34.00 | 35.87 | 29.14 | 33.97 |
| PC40B | 49.19 | 48.39 | 35.55 | 44.16 |
| PH210T | 36.32 | --- | 25.76 | 31.09 |
| PH210B | 38.14 | 47.04 | 31.43 | 40.42 |
| PH410T | 34.00 | 35.87 | 29.14 | 33.97 |
| PH410B | 49.19 | 48.39 | 35.55 | 44.16 |
| PH413T | 33.93 | 36.10 | 35.06 | 38.81 |
| PH413B | 53.33 | 53.45 | 42.77 | 50.45 |
| PH416T | 41.31 | 44.30 | 42.66 | 45.23 |
| PH416B | 55.89 | --- | 52.04 | 58.80 |

τ_{uexp} : bond stress of sheath from the test data
 τ_{ucm} : bond stress calculated by using Fujii-Morita's equation
 τ_{ucoj} : bond stress calculated by using Orangun-Jirsa-Breen's equation

Six specimens were tested under repeated loading. First, the specimens were loaded with incremental of 1 tonf until it reached 2/3 of the level of 1.1, 1.3, and 1.5 times the value of the specified yield strength of the main bars. The reason of multiplying the value of 2/3, is because a lapping length of 20d was tested, while the design lapping length is 30d. Then, after 10 cycles of repeated loads with the same level in each case, the maximum loads were obtained. Same as in the monotonic loading, the bottom bars yielded before the bond failure was obtained, while the top bars failed in bond before the bars yielded.

The following testing pattern was adopted for two specimens with the same parameter: first the top bar was tested until the specimen was close to failure. Then the bottom bar was tested until it failed, then the bottom bar of the second specimen was tested until the load was close to the maximum load, so after that the top bar was tested until failure. By this testing pattern the authors tried to get good results with the limited number of specimens in each case.

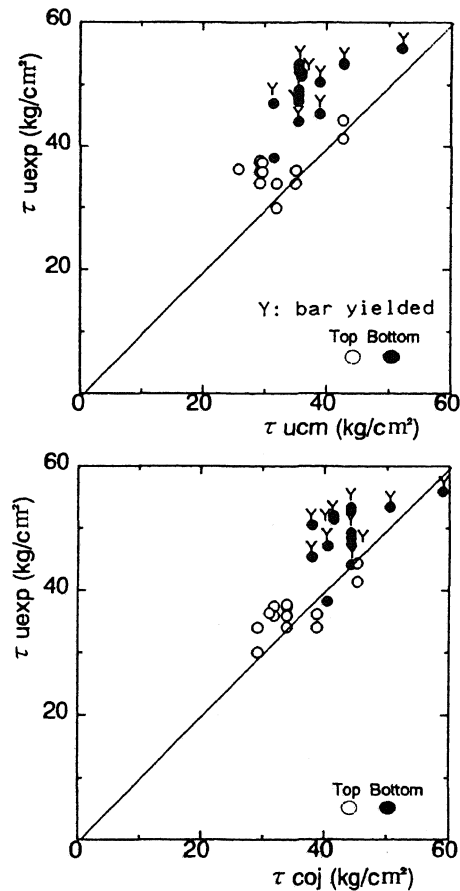


Figure 4. Experimental and calculated bond strengths

4. TEST RESULTS

The system of main bar-grouted mortar-sheath behaved as a single unit, and all the top bars failed in bond at the sheath surface. The bottom bars also failed in bond at the sheath surface after the yielding of main bars.

Relations for all test specimens between lapping lengths, bond stresses, and main stresses at the maximum loads are illustrated in the following figures. These diagrams were deduced by converting applied maximum forces into bond stresses using Eq. (1). Also, bond splitting strength calculated by the formulas proposed by Fujii-Morita (Fujii 1979) Eq. (2) and Orangun-Jirsa-Breen (Orangun 1977) Eq. (3) are plotted in every case.

Equation (2) was derived for continuous bars from the bond splitting failure, while equation (3) was derived for bars with lapping splices.

$$\tau_{uexp} = \frac{P_{max}}{l_s \cdot \phi} \quad (1)$$

$$\tau_{ucm} = (0.307bi + 0.427 + 24.9 \frac{k A_{st}}{s N_t d_b}) \sqrt{\sigma_g} \quad (2)$$

multiplied by 1.22 for bottom bars

$$\tau_{ucoj} = (1.2 + 3C + 50d_b + \frac{A_{st} w \sigma_y}{35.2 N_t s d_b}) \times 0.265 \sqrt{\sigma_g} \quad (3)$$

divided by 1.3 for top bars

where:

- P_{max}: maximum force in the main bar;
- φ: perimeter of sheath;
- l_s: lapped length;
- b_i: parameter for the failure of concrete;
- k: parameter of the lateral reinforcement;
- A_{st}=A_w: area of lateral reinforcement;
- N_t: total number of main bars;
- d_b: diameter of sheath;
- wσ_y: yielding strength of lateral reinf. ;
- C: half clear spacing between bars or half available concrete width per bar or splice resisting splitting in the failure plane;
- σ_g: concrete cylinder strength.

The experimental bond strength τ_u and the calculated bond strength are compared in Table 5 and Figure 4. The test results disagree with the bond strengths calculated by the Fujii-Morita's formula, while most of the test results agrees well with the bond strength calculated by the Orangun-Jirsa-Breen's formula, but disagree with some of the test results from the bottom which yielded before the bond failure.

4.1 Influence of the height of lug

First transverse cracks appeared at 1/3 the specimen length at 6 tonf in all cases. The first cracking loads for the bottom bars were 1.3 times those for the top bars. At 9 tonf transverse cracks developed at the center, at 12 tonf cracks developed in the longitudinal direction at both ends. Cracks spread with the increment of load and before the maximum load a concentration of cracks at the corners was observed.

- σ : Normal Stress in Main Bar (tf/cm²)
- τ_b : Bond Stress in Main Bar (kgf/cm²)
- τ_s : Bond Stress in Sheath (kgf/cm²)
- τ_{lb} : Bond Stress in Lapping Bars (kgf/cm²)

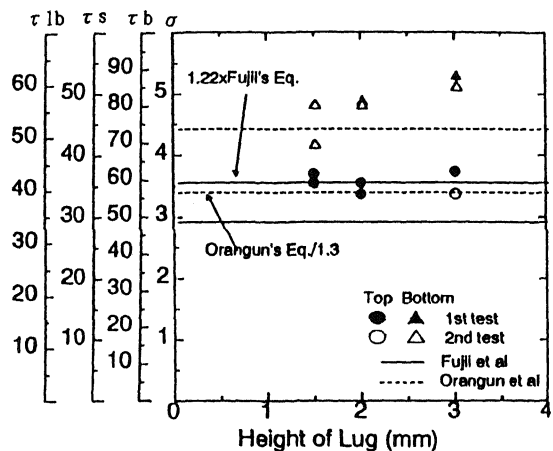


Figure 5. Relationship between joint strengths and lug heights of sheaths

Figure 5 shows the relation between the normal stresses in main bar, average bond stresses in main bar, sheath, lapping bar at the maximum loads and the lug heights. The maximum loads for the bottom bars were 1.38 times bigger than for the top bars.

An increment in the bar stress of the bottom bars with the increment of the height of the sheath lug is observed, while for the top bars which failed in bond at the sheath surface, the main bar stress remained almost constant. In this figure the Orangun-Jirsa-Breen equation shows a good agreement with the test results, while the Fujii-Morita equation give lower calculated values than the test results, where the calculated values for the bottom bars agree well with the top bars test results. Even though, the height of the sheath lug has no influence in both formulas, the Orangun-Jirsa-Breen equation almost fits with this experiment.

4.2 Thickness of the cover concrete

The first cracks appeared at 4 tonf and 6 tonf for the top and bottom bars,

respectively. An increment of the number of cracks with the decrement of the cover concrete was observed. For specimens with cover concrete of 40 mm transverse cracks were distributed at 1/3 the length of the specimens. Specimens with cover concrete of 30 mm had a similar crack pattern to that with cover concrete of 40 mm, except that the transverse cracks were distributed at 1/4 of the specimens length. No differences of the crack patterns between the top and bottom bars were observed.

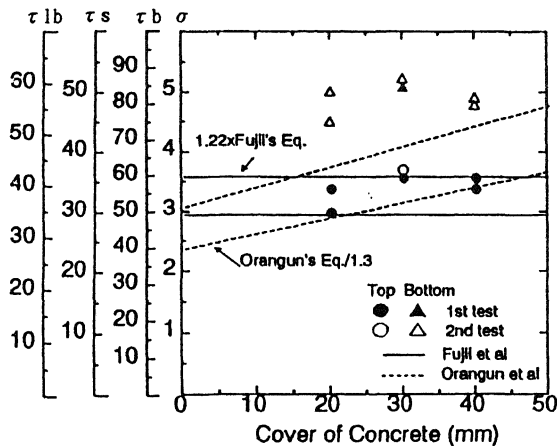


Figure 6. Relationship between joint strengths and thickness of cover concrete

Figure 6 shows the relation between the lapping joint strengths and the cover thickness of concrete. An increment in the strength for the cover concrete of 20 and 30 mm, while a decrement for the strength of 40 mm is appreciated. This decrement in the strength is assumed to be related with the lower concrete strength of the specimen. The maximum loads for the bottom bars were 1.44 times bigger than for the top bars.

In this figure, a good agreement of the test results from the top bars with the Orangun-Jirsa-Breen's equation can be appreciated, while disagree with the test results from the bottom bars. Here again, the Fujii-Morita calculated data for the bottom bars agrees well with the test results from the top bars. During this experiment according to Fujii-Morita, a side split bond failure was observed, by this reason in Figure 8 the calculated value from using Fujii-Morita equation remains almost constant.

4.3 Lateral reinforcement

The first cracks for the top bars appeared at 5 tonf in the central part of the specimen, while for the bottom bars appeared at 7 tonf at 1/3 the specimen

length. For the specimens with 2-D10 as lateral reinforcement, just before failure a transverse crack appeared at the end of the lapping length, and the failure pattern due to the splitting of the side bars. For specimens with 4-D10 and 4-D13, the crack pattern was almost similar to each other and failure was due to the corner bar split. During the testing of the top bars of specimens with lateral reinforcement of 4-D16 the specimens were broken at the half of the specimen length (where the main bars abutted), with a less number of cracks than in the other cases. No damage was observed for the bottom bars.

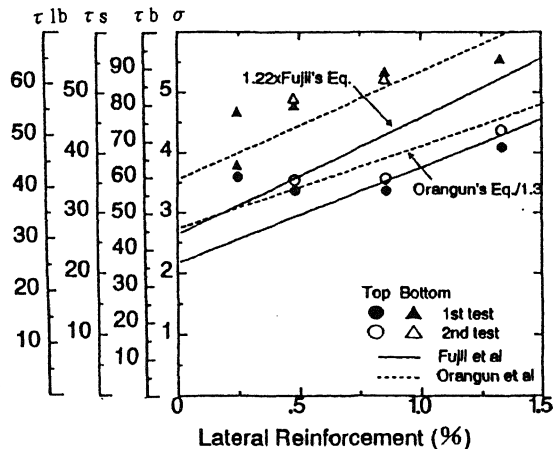


Figure 7. Relationship between joint strengths and the lateral reinforcement ratios P_w

Figure 7 shows the relation between the joint strengths and the lateral reinforcement ratios. An increment in the strength with the increment of the lateral reinforcement ratio is appreciated for the bottom bars, while the same increment is not recognized for the top bars. Here, the strength for the lateral reinforcement for 2-D10 is higher than the others because its concrete strength is also higher in a 3%.

The maximum loads for the bottom bars were 1.38 times bigger than for the top bars. In this figure, the Orangun-Jirsa-Breen's equation shows a good agreement with either the top or bottom tests results, while the calculated values from the Fujii-Morita equations for the top bars are close to the test results. From here, even the main reinforcement are not continuous bars this system proves to be good enough to transfer the stress from each bar and then to the surrounding concrete.

4.4 Loading history

Figure 8 shows the relationship between the number of times the specimens were loaded

and the normal stress in main bar. average bond strengths at the maximum load.

This figure shows that the bottom bars reached the maximum load after ten loading cycles were completed, while for the top bars only the specimens tested at 1.1 times the yielding strength reached the maximum load after the ten cycles were completed.

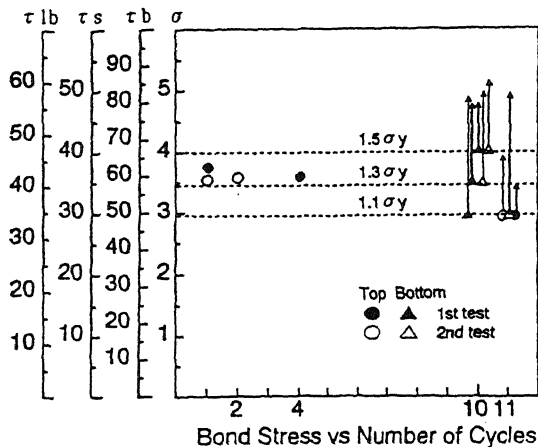


Figure 8. Relationship between the normal stress in main bar and the number of loading cycles

The other specimens failed at approximately 18 tonf, which correspond to 1.3 times the yielding strength of bars with a lapping length of 30d.

No differences were appreciated concerning the variation of the repeated loads, where either the top or bottom bars showed a similar behavior to the specimens under the monotonic loading.

5. CONCLUSIONS

From the foregoing discussions, the following conclusions can be obtained.

- 1) Even the main reinforcement are not continuous bars this system proves to be good enough to transfer the stress from each bar and then to the surrounding concrete.
- 2) With the same lapping length, a difference of the lapping joint strength for the top and bottom bars was recognized.
- 3) An improvement in the bond strength is recognized with the increment of the lug height of the sheath.
- 4) No remarkable influence from the thickness of cover concrete was recognized.

5) An increment of the joint strength with the increment of the lateral reinforcement ratio was appreciated for the bottom bars, while for the top bars it was almost constant.

6) A decrement of the average bond stresses at the maximum load with the increment of the lapping length are observed. A lapping length of 20d is recognized to be good enough for the bottom bars, but also this length is not enough for the top bars. For the real design a lapping length of 30d is proposed in order to avoid bond failure.

7) During repeated loading the degradation of bond strength and bond stiffness depended on the maximum load reached previously.

REFERENCES

- Imai, H.; Yamaguchi, T.; Yanez, R., "Bond Performance of a Lapping Joint Developed for Precast Concrete Columns", Proceedings of The Japan Concrete Institute, Vol. 13, No 2, 1991, pp. 1063-1068.
- Fujii, S.; Morita, S., "Splitting Bond Capacity of Deformed Bars (Part 2), A Proposed Ultimate Strength Equation for Splitting Bond Failure (in Japanese)", Transactions AIJ, No. 324, Feb. 1983, pp. 45-53.
- Orangun, C.O.; Jirsa, J.O.; Breen, J.E., "A Reevaluation of Test Data on Development Length and Splices", ACI Journal, Vol 74, March, 1977, pp. 114-122.
- Kemp, E.L.; Wilhelm, W.J., "Investigation of the Parameters Influencing Bond Cracking", ACI JOURNAL, Proceedings V.76, No. 1, January 1979, pp. 47-71.
- Morita, S.; Kaku, T., "Splitting Bond Failures of Large Deformed Reinforcing Bars", ACI JOURNAL, Proceedings V.76, No. 1, January 1979, pp. 93-110.
- Castro, J.; J.; Yamaguchi, T.; Imai, H., "Seismic Performance of Precast Concrete Beam Column Joints", Proceedings of the Tenth World Conference on Earthquake Engineering, Madrid, 1992.
- Imai, H.; Yamaguchi, T.; Kobayashi, T., "Seismic Performance of Precast Concrete Columns With Lapping Joints Under Shear Forces", Proceedings of the Tenth World Conference on Earthquake Engineering, Madrid, 1992.